

RESEARCH PAPER

## Insight into the Uranium Biosorption from Aqueous Solution by Biomass Immobilization

Meisam Sadeghi <sup>1,\*</sup>, Zahra Moghimifar <sup>2</sup>

<sup>1</sup> Nanotechnology Research Institute, Faculty of Chemical Engineering, Babol Noshirvani University of Technology, Babol, Iran

<sup>2</sup> Faculty of Chemical and petroleum Engineering, Chemistry and Chemical Engineering Research Center of Iran (CCERCI), Tehran, Iran

### ARTICLE INFO

#### Article History:

Received 09 July 2021

Accepted 18 September 2021

Published 15 October 2021

#### Keywords:

Biosorption

Saccharomyces Cerevisiae

Uranium

Zeolite Clinoptilolite

Equilibrium and Distribution

### ABSTRACT

Uranium is one of the most threatening elements due to its radioactivity and high toxicity, and significant amounts of it are released into the environment in the course of nuclear fuel cycles. In this regard, biosorption technology offers the advantages of low operating costs and high efficiency in metal removal from aqueous solutions. This work evaluated the sorption of uranyl ions from aqueous solutions by *Saccharomyces Cerevisiae* (SC) on zeolite clinoptilolite. First, natural zeolite was characterized by classical chemical analysis, and then the influence of solution pH, temperature, contact time, and initial concentration on the sorption of uranyl were investigated. The concentration range of uranyl in the solution was between 0.02 and 1 mmol L<sup>-1</sup>, which was determined by the inductively coupled plasma optical emission spectrometry (ICP-OES). In addition, the results showed that metal binding occurred extracellularly at the cell wall surface and the sorption rate of uranyl ions by free yeast cells was rapid from SC. Further, comparing the results from BET for the primary and modified biomass showed an increase in the surface area of the modified biomass as a result of adsorption on clinoptilolite zeolite. The equilibrium adsorption ratio and distribution of uranium hydrolysis products for all samples were calculated, indicating that the points corresponding to initial concentrations of less than 0.1 mmol L<sup>-1</sup> have higher and narrower absorption fractions. Furthermore, the adsorption rate decreased at concentrations higher than 0.2 mmol L<sup>-1</sup> compared to low concentrations.

### How to cite this article

Sadeghi M, Moghimifar Z. *Insight into the Uranium Biosorption from Aqueous Solution by Biomass Immobilization*. *Nanochem Res*, 2021; 6(2):256-267. DOI: 10.22036/ncr.2021.02.012

### INTRODUCTION

Different types of exchangers such as zeolites have widespread and important applications, especially in the nuclear waste recycling industry [1, 2]. Various methods have been applied to treat nuclear wastewater due to its widespread nature and the heavy metals that it contains [3-7]. Conventional technologies for reducing heavy metal contamination

mainly involve the following methods alone or in combination: evaporation, chemical separation, and adsorption, ion exchange, and membrane processes [8-10]. In addition, various parameters are involved in selecting a wastewater treatment method, such as the initial cost of the equipment used, operating cost of the process, minimizing the volume of residual waste, etc. [11, 12]. Research results have shown that using biological materials

\* Corresponding Author Email: [meisam\\_Sadeghi1363@yahoo.com](mailto:meisam_Sadeghi1363@yahoo.com)  
[m-sadeghi@nlai.ir](mailto:m-sadeghi@nlai.ir)



This work is licensed under the Creative Commons Attribution 4.0 International License.

To view a copy of this license, visit <http://creativecommons.org/licenses/by/4.0/>.

is an economically and environmentally suitable option for the removal and recovery of heavy metals from aqueous solutions, which is called biosorption technology [13-16]. Biosorption is a property of certain types of non-living microbial biomass to absorb and concentrate heavy metal ions from their very dilute aqueous solution (Fig.1). In summary, the main advantages of this technology include high efficiency at low metal concentrations,

performance over a wide temperature and pH range, easy recycling of biosorbents, availability of cheap and accessible biomass resources, and low cost of the adsorption and recycling process [17, 18]. Bacteria, fungi, algae, and some plants have different types of biomasses which have good potential for adsorption of heavy metals [19]. The adsorption of uranium by different immobilized microorganisms is reviewed in Table 1.

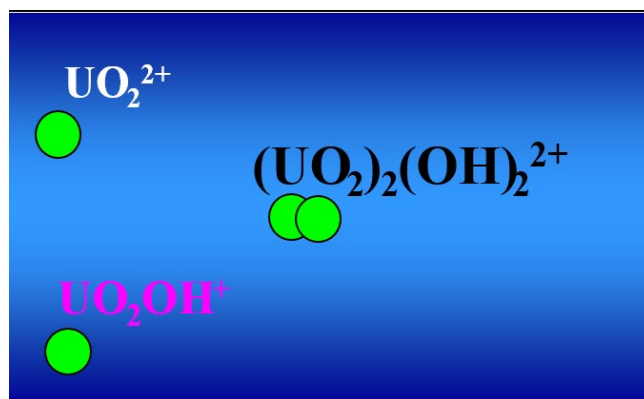


Fig. 1. An ionic scheme for uranium hydrolysis products in solution

Table 1. Adsorption of uranium by immobilized microorganisms

Series No	Adsorbent	Adsorption Efficiency	Equilibrium study	Analysis method
1	<i>Myxococcus xanthus</i>	95.99%	Langmuir model	ICP
2	<i>Sargassum fluitans</i>	560 mg/g,	Langmuir model	ICP-AES
3	<i>Trametes versicolor</i>	158.0 - 309.1 mg /g	Langmuir	Sodium salicylate
4	<i>Microcystis aeruginosa</i>	48 mg/g	Langmuir	ICP-AES
5	<i>Lentinus sajorcaju</i>	378 mg/g	Freundlich	spectrophotometric method
6	<i>Trichoderma harzianum</i>	612 mg/g	Langmuir model	Arsenazo (III) method
7	<i>Catenella repens (a red alga)</i>	303 mg/g	Freundlich isotherms	Arsenazo (III) method
8	<i>Cytoseria indica</i>	233 mg /g	Langmuir isotherm	ICP-AES
9	<i>Citrobacter freundii</i>	48.02 mg/g	Freundlich	Titanium trichloride titration
10	<i>Ganoderma lucidum</i>	8.98 mg/g	-	-
11	<i>Pseudomonas putida</i>	88.4%	Langmuir equation	-
12	Immobilized <i>Aspergillus</i>	98.4 mg/g	Freunlich and Temkin isothermal	-
13	<i>Penicillium citrinum</i>	127.3mg/g	Freundlich isotherm	Arsenazo (III) method
14	<i>Pleurotus mutilus</i>	636.9 mg/ g	Langmuir isotherm	XRF spectrometer

Most separation and purification processes that use the adsorption technology apply a constant bed column with continuous flow [20]. By analyzing the initial concentrations of the column as a function of time-pH or volume of column output, the efficiency with performance of the fixed bed column is obtained [21].

The objective of this study was the removal and recovery of uranium ions (the major heavy metal in nuclear industry wastewater) by SC, a species of brown algae, in a packed bed column. In this work, a natural zeolite called clinoptilolite from Semnan mines was selected for separating U (VI) ions and characterized by differential thermogravimetry (DTG). Further, the influence of variables such as the initial concentration, pH, and contact time between the exchanger and solution phase on the adsorption of U (VI) ions was investigated and optimized.

## MATERIALS AND METHOD

In this study, yeast from SC was used as a biological adsorbent. The SC strain used in these experiments was PTCC 5052, produced by Collection Center of Scientific and Industrial Research Organization in Iran. The maintenance of the strain is crucial since the microorganism used must maintain its desired properties over time. To obtain the strain, SC was cultured in a pre-sterilized yeast peptone dextrose (YPD) liquid medium for 48 h at 28 °C. YPD was prepared as follows: 20 g L<sup>-1</sup> peptone (Quelab), 20 g L<sup>-1</sup> glucose monohydrate (Carl Roth), and 10 g L<sup>-1</sup> yeast extracts (Merck) [22]. The zeolite deposit is clinoptilolite and was obtained from Semnan mines in northeastern Iran. In addition, the zeolite particles were granulated using standard laboratory sieves in sizes of 425-200 µm, corresponding to a mesh size of 40-70 in the ASTM standard system, and heated at 400 °C for 60 min. After heating, it was cooled to room temperature and kept in a desiccator with silica gel for immobilization and adsorption tests. The heating process was carried out in order for zeolite cavities to lose water and prepare the zeolite particles before conducting the experimental tests.

## EXPERIMENTAL DETAILS

### *Preparation of the uranyl solution*

For the preparation of the uranyl solutions, different types of uranyl stock solutions (1 mmol L<sup>-1</sup> UO<sub>2</sub><sup>+2</sup>) were prepared at the required stoichiometric concentration by dissolving different amounts of

uranyl nitrate salt (UO<sub>2</sub>(NO<sub>3</sub>)<sub>2</sub>·6H<sub>2</sub>O) in distilled water. The stock solution was utilized at different concentrations, and the initial pH of the uranyl solution was adjusted to the desired value by adding 0.1 N HNO<sub>3</sub> or 0.1 N NaOH.

### *Uranyl Equilibrium adsorption experiment before immobilization*

This study aimed to compare the sorption of free and immobilized cells and evaluate the mechanism of the biological sorption process of UO<sub>2</sub><sup>+2</sup> by SC yeast. The same values and test conditions were used for comparison. Further, the concentration of uranyl ions in the solution was determined by inductively coupled plasma optical emission spectroscopy, ICP-OES Optima 7300DV, PerkinElmer, USA.

The sorption (q) at equilibrium was calculated for each sample using the following equation:

$$q = V(C_i - C_f) / m$$

The percentage of equilibrium sorption is determined by using the following equation:

$$EA(\%) = 100(C_i - C_f) / C_i$$

Where V stands for the sample volume (L), C<sub>i</sub> and C<sub>f</sub> are the initial and final concentrations of uranyl (mmol L<sup>-1</sup>), respectively; m denotes the dry mass of sorbent (g), and q represents the amount of ions adsorbed per unit mass of sorbent at the equilibrium time (mmol g<sup>-1</sup>).

### *Immobilization of SC*

SC yeast grown in a YPD agar medium was first cultured in a 250 mL conical flask containing 50 mL of aseptic YPD nutrient medium and incubated in a rotary shaker at 28 °C and 160 rpm for two days. After that, 1 mL of SC, containing 60 mL of aseptic liquid culture solution and 20 mL of zeolite (equivalent to 2.34 g of zeolite), was transferred to 250 mL of Erlenmeyer flasks and incubated in a rotary shaker at 25 °C and 130 rpm for 3 days. At this stage, the free yeast cells were transferred to and grew on the zeolite particles. To separate the immobilized cells, a centrifuge was then used at a low speed of 1200 rpm for 20 min. The supernatant was transferred to an aseptic container for cell counting under aseptic conditions and the remainder was stored at 50 °C for two days to be dried. Then, a portion of the supernatant from

centrifugation of the immobilized cells and a portion of the cells that grew in the YPD medium after two days were selected and the number of cells immobilized on the zeolite support was determined by cell counting. To count the number of yeast cells grown for two days, the solutions were first diluted 10-fold and 100-fold and counted on the diluted solutions due to the large accumulation of cells.

#### *Uranyl Equilibrium adsorption experiment after immobilization*

In the following equation,  $q$  denotes the mmol of uranyl ions adsorbed per gram of fixed yeast adsorbent:

$$q = V (C_{f(\text{blank})} - C_f) / m$$

Where  $C_{f(\text{blank})}$  represents the equilibrium concentration of uranyl after adding crude zeolite to the solution, and  $C_f$  is the equilibrium concentration of uranyl after adding the cell immobilized on the zeolite to the solution.

#### *Genetic algorithm for the biosorption process*

The genetic algorithm is applied to obtain the optimal parameter values by minimizing the output error between the experimental and simulated output data. This section deals with the estimation of parameters for the growth of SC in MBR. In this work, mathematical modeling techniques were used to study the sorption of  $\text{UO}_2^{+2}$  in the MBR operating system in batch mode, and the proposed model describes cell growth, substrate concentration, and  $\text{UO}_2^{+2}$  sorption. The mathematical model was derived from the principles of mass and energy balance in which the mass balance was first applied around the bioreactors and the general differential equations were used to describe the concentration of  $\text{UO}_2^{+2}$  sorption and the consumed glucose substrate. Furthermore, the microorganisms SC were set up as a function of time and dilution rate in batch and continuous modes, respectively. The mathematical modeling was based on the kinetic models of logistic, Tessier, Monod, Moser and Contois. The proposed kinetic models were applied to the obtained equations, and the coefficients corresponding to these models were considered as variables and optimized. The final equations, describing the batch operation and consisting of 7 to 9 variables with respect to the applied model, were solved simultaneously by applying a genetic algorithm.

#### *Optimization of Uranyl Equilibrium adsorption experiment*

Firstly, 50 mL of uranyl solutions with initial concentrations ranging from 0.02 to 1 mmol  $\text{L}^{-1}$  were prepared. Then 20 mg of yeast adsorbent was added to the solutions and incubated at room temperatures for 4 h to study the uranyl sorption. After the filtration of the mixture, the filtrate containing uranyl ions was measured and the effect of time and pH were evaluated.

##### *(a) Effect of time and pH*

The pH and temperature of the solution were adjusted to 4 and 25 °C, respectively. By adding 20 mg of yeast adsorbent to the solutions, the samples were incubated at 200 rpm for a contact time of 6 h and at different pH values from 3 to 6. The samples were then allowed to absorb uranium. To separate the adsorbed uranyl ions, the supernatant was centrifuged at a speed of 9000 rpm for 10 min. Finally, the time-pH dependence of uranium biosorption on the immobilized biomass was investigated.

##### *(b) Effect of bed volume*

Uranium adsorption was evaluated at SC biomass immobilized on zeolite. Experiments were performed in fixed-bed mode using 100 mg/L uranium solution at bed depths equal to 80 cm.

#### *BET analysis*

To observe the effect of clinoptilolite zeolite on the specific surface area of biomass, the BET assay was performed for the primary biomass and modified biomass (adsorbed cells on zeolite), respectively.

## **RESULTS AND DISCUSSIONS**

#### *Thermal stability of clinoptilolite*

The thermal decomposition method was applied to measure the amount of water and other volatiles in the samples by reducing the weight of the sample. The temperature was studied over the range of 25 to 900 °C, and the rate of temperature change was 10 °C  $\text{min}^{-1}$ . The thermal curve for natural zeolite of clinoptilolite is shown in Fig. 2, in which an index peak can be seen in the temperature range of 25-200 °C, indicating a weight loss percentage of 1.13% which is due to the removal of water molecules. In fact, weakly-bound water molecules are released in this range.

The escape of the water molecules is noticeable

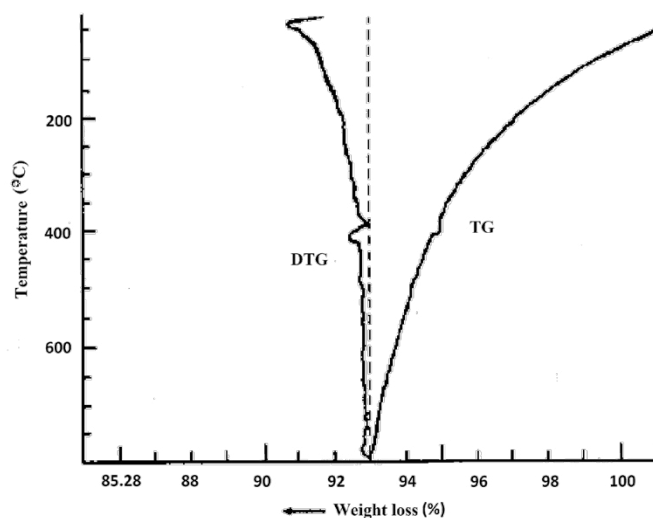


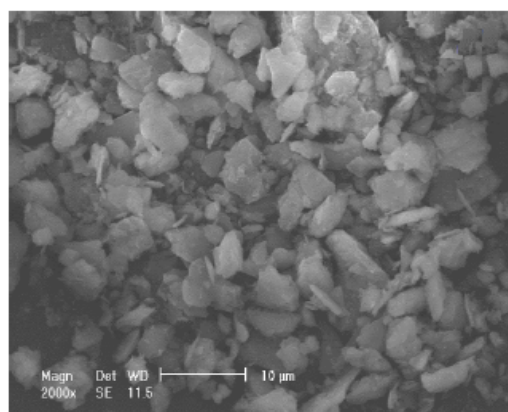
Fig. 2. DTG/TG spectrum of the zeolite type of clinoptilolite

and occurs very rapidly. In the temperature range of 200 to 300 °C, the slope of the thermocurve decreases and the escape of water molecules becomes slower but continuous. Above 400 °C, this speed slows down even more and the water molecules gradually leave the zeolite bed. In practice, the amount of water leaving the zeolite structure can be an appropriate criterion for adsorption capacity, since the released water molecules can be delivered to other molecules. Heating the sample expels the water molecules trapped in the zeolite channels and cavities as well as the adsorbed water molecules from the system.

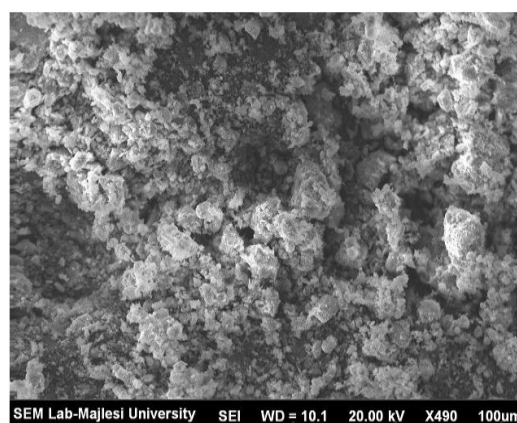
#### Immobilization of yeast cells on clinoptilolite

The characterization of the zeolite surface is determined by SEM. Secondary Electron Imaging type detector (SEI) was used for imaging SEM (Fig. 3).

Fig. 3a shows the images of crystalline structure of acid leached zeolite without cells, and Fig. 3b demonstrates the morphology of zeolite loaded with cells. A comparison of Fig. 3a and 3b indicates that the surface structure of the zeolite has changed and the voids in the zeolite have become loaded with cells. Additionally, the proliferation of yeast cells that grew on the zeolite support was clearly maintained. In conclusion, the SEM photographs confirm the main assumptions of this study that the trapped nutrients above the cavities were used by the immobilized SC cells for biomass production.



(a)



(b)

Fig. 3. (a) Scanning electron micrograph of natural clinoptilolite (b) Scanning electron micrograph of clinoptilolite with immobilized yeast cells

#### Spectrum of uranium with ICP-OES technique

The calculated number of immobilized SC cells per support was  $17.1 \times 10^8$  cells ml<sup>-1</sup>. Fig. 4 shows a sample of the uranium measurement spectrum with an ICP-OES device. All quantitative measurements of uranium in this paper were taken at 409 nm.

#### Genetic algorithm for the biosorption process

The results of the applied kinetic models, i.e., the logistic, Monod, Moser, Tessier and Contois models, were in good agreement with the experimental data (Table 2). Among the considered models, the logistic model showed the best performance for the MBR in batch mode with a regression value of 0.9958. Considering the obtained results, which are closely comparable with the experimental data, the models implemented with the optimized coefficients can be efficiently applied to predict the concentrations of the different components involved in  $UO_2^{+2}$  sorption using glucose substrate and SC microorganisms (Fig. 5). The great advantage of this technique is the ability of the models to predict the behavior of the system without experimental studies.

#### Optimization of uranium ion adsorption with free and immobilized yeast adsorbent

##### (a) Influence of time and pH

The interaction of the cell wall groups containing carboxyl, amine, and amide groups with the uranyl ion in solution was dependent on the amount of protonated functional group present on the biosorbent, which in turn depended on the pH. Based on the two results obtained from the pH-dependent protonation status of the functional groups on the cell surface and the nature of the metal species present in the solution, pH = 4 was selected as the optimum pH for the biosorption of uranyl. Moreover, several studies on uranium sorption by different types of adsorbents showed that the adsorption behavior is similar in the defined pH range. When the effect of pH on the sorption of uranyl ions by immobilized SC cells was studied, pH = 4 was again identified for the maximum adsorption (Fig. 6). However, in this case, the changes in adsorption as a function of pH are not significant compared to the free cells.

The influence of pH and time on the adsorption capacity of  $UO_2^{+2}$  by the sorbent is shown in Fig.

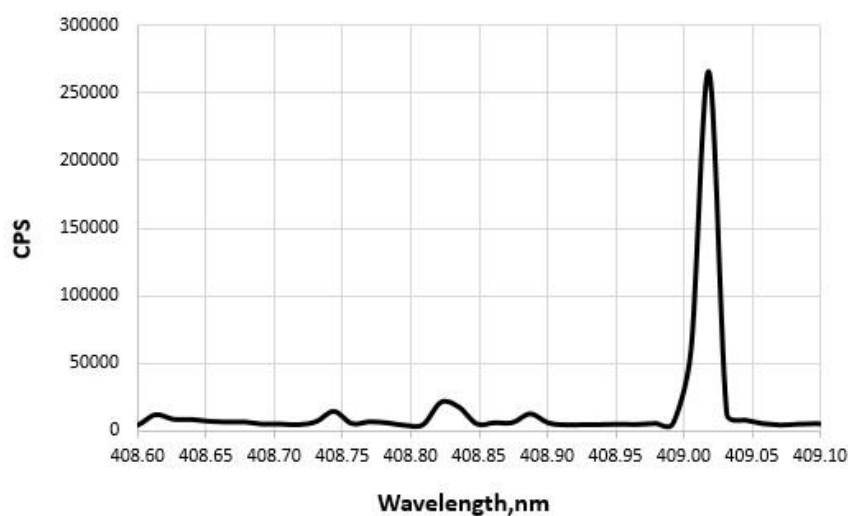


Fig. 4. Measurement spectrum of uranium with ICP-OES technique at 409 nm

Table 2. Kinetic mathematical model parameters for MBR

Parameters		Ksp (gL <sup>-1</sup> )	Kss (gL <sup>-1</sup> )	Ksx (gL <sup>-1</sup> )	μ <sub>m</sub> (h <sup>-1</sup> )	R <sup>2</sup>
Mathematical Models	Logistic	0.98	1.321	0.47	15.67	0.9958
	Tessier	15.02	28.94	22.08	0.49	0.9904
	Monod	13.02	17.46	8.99	0.47	0.9874
	Moser	25.85	28.43	42.53	1.40	0.9912
	Contois	9.09	11.30	29.66	0.58	0.9801

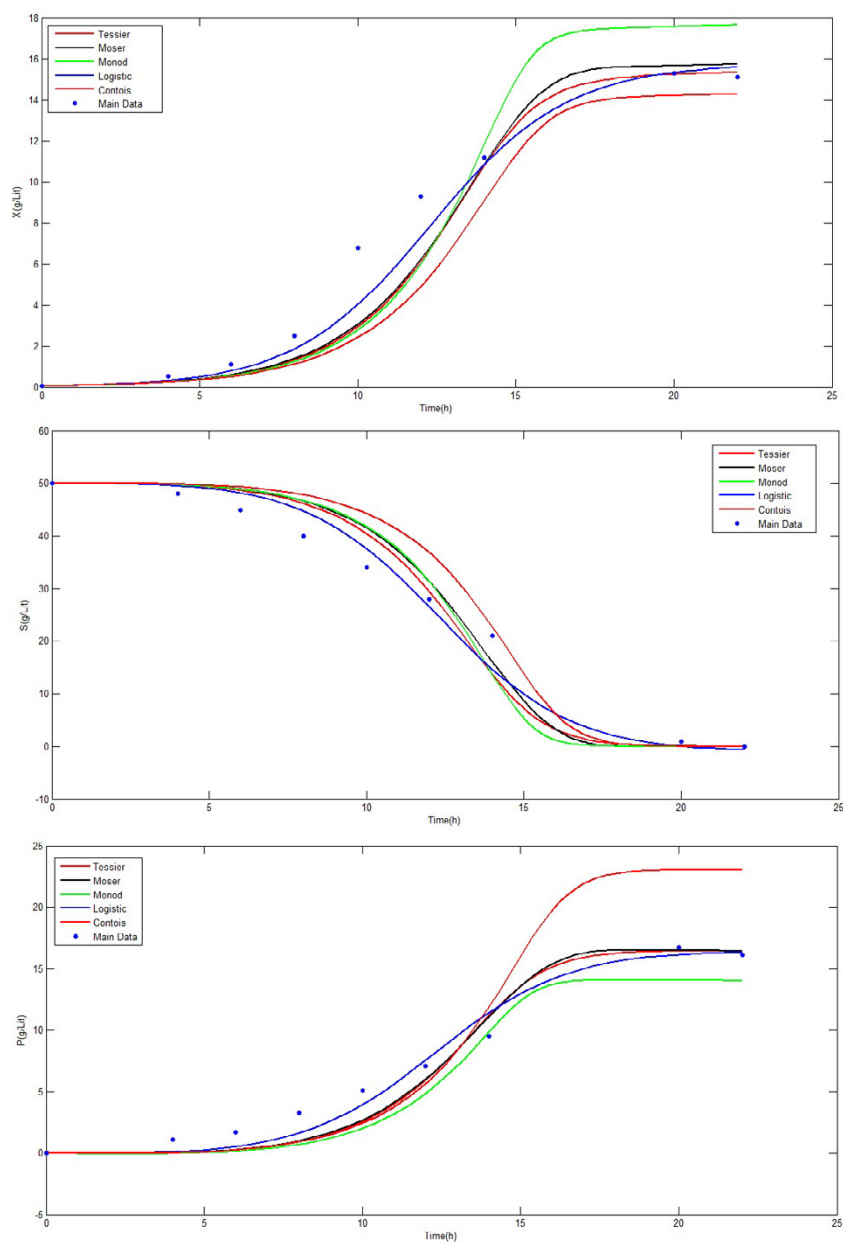


Fig. 5. Prediction of different models for (a) microorganisms, (b) substrates and (c) biosorption product in batch membrane reactors.

7. The biosorption of metal ions from the solution occurs rapidly in the initial phase, and the results indicate that the biosorption of uranyl ions is fast and  $UO_2^{+2}$  ions are removed up to 90% in the first 30 min of sorption. The rapid phase is probably due to the high number of available active adsorption sites on the biomass cell wall. By the passage of time, the active binding sites became saturated, and a slowdown occurred. Then, equilibrium was established after 4 h and this time was chosen as the

contact time for further experiments.

(b) Influence of bed volume on uranyl ion concentration

The dependence of the initial concentration of  $UO_2^{+2}$  adsorption on the sorbent is shown in Fig. 8. At low concentrations of  $UO_2^{+2}$ , the adsorption increases rapidly with increasing concentration, while at high concentrations, the adsorption rate increases slowly. Finally, the adsorbent is saturated

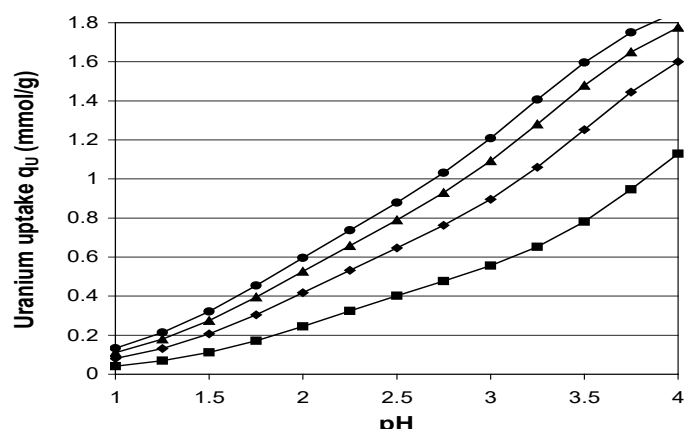


Fig. 6. Influence of solution pH on the uranium sorption at fixed uranium equilibrium concentration

(●)  $U_f = 6.0$  (mmol/g); (○)  $U_f = 4.0$  (mmol/g);  
(△)  $U_f = 2.0$  (mmol/g); (■)  $U_f = 0.5$  (mmol/g);

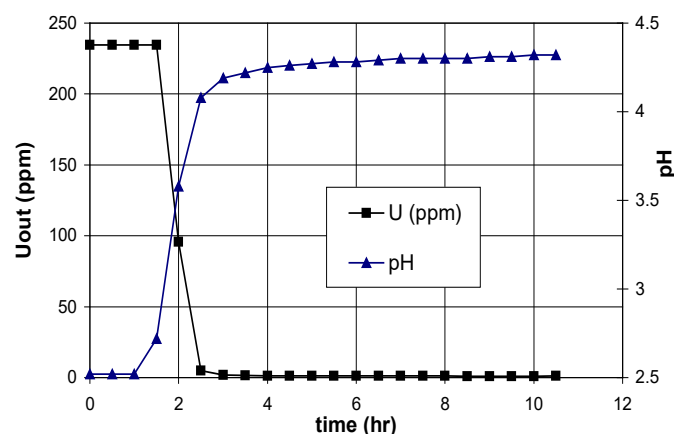


Fig. 7. Response of the column outlet concentration to the step function in the column inlet;  $F=175$  ml/h,  $V_{bed}=280$  ml, biomass = 22.64 g

by an increase in the concentration of  $UO_2^{+2}$  which is due to the fact that the suitable active sites gradually decrease with increasing uranyl ions.

Additionally, the effect of Residuals of experimental and the Mass Transfer Model calculated on the breakthrough characteristics of the fixed bed sorption system were identified. As shown in Fig. 8, the adsorption rate of metal ions increases relatively steeply at low concentrations. However, at high concentrations, the adsorption rate increases with a small slope as the available active sites gradually decrease with increasing the concentration.

#### Calculation of the equilibrium absorption ratio

The percentage of equilibrium adsorption was calculated and plotted by using Helmholtz Integral Equation Method (HIEM) model regression for all

of the samples. As can be seen in Fig. 9, the points corresponding to initial concentrations of less than about  $0.1 \text{ mmol L}^{-1}$  have a higher and closer absorption percentage.

In the concentration range of  $0.0$  to  $6.0 \text{ mmol/L}$ , the difference between the initial and equilibrium concentrations ( $C_i - C_f$ ) is closer to the value of  $C_f$  due to the very small amount of  $C_i$ , which indicates a higher adsorption (see Fig. 10). However, at concentrations above  $0.2 \text{ mmol L}^{-1}$ , the adsorption rate decreases compared to low concentrations.

#### Distribution of uranium hydrolysis products

The hydrolysis of uranium (VI) has been investigated in  $0.10 \text{ mol dm}^{-3} \text{ NaClO}_4$  and  $\text{KCl}$  and  $1.0 \text{ mol dm}^{-3} \text{ KNO}_3$  by applying the potentiometric technique (Fig. 11).

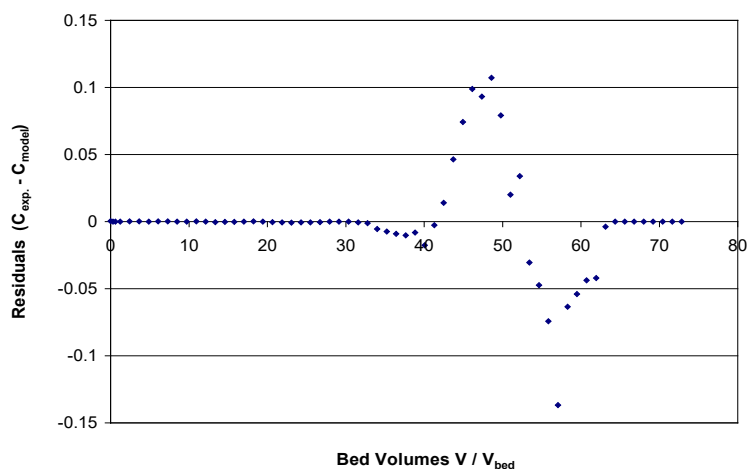


Fig. 8. Residuals of experimental and the Mass Transfer Model calculated uranium breakthrough curve.

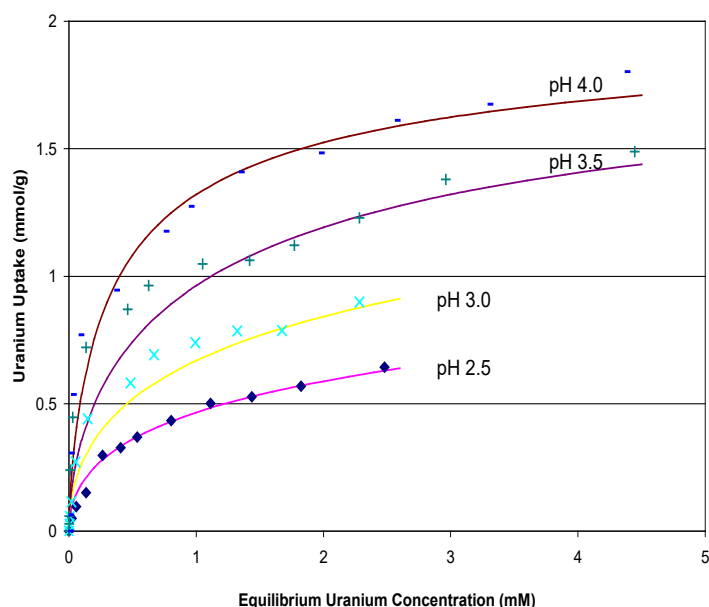


Fig. 9. Comparison of experimental uranium isotherms and HIEM calculation at different solution pH

The species  $\text{UO}_2\text{OH}^+$ ,  $(\text{UO}_2)_2(\text{OH})_2^{2+}$ ,  $(\text{UO}_2)_3(\text{OH})_4^{2+}$ ,  $(\text{UO}_2)_3(\text{OH})_5^{3+}$  and  $(\text{UO}_2)_4(\text{OH})_7^{7+}$  have been identified in nitrate media, and all of these species (except for  $(\text{UO}_2)_4(\text{OH})_7^{7+}$ ) have also been identified in chloride and perchlorate media (Fig. 12).

The differences in the complexation behaviour in the media may be due to oxoanion binding by the nitrate, a process which has also been observed for sulfate (Fig. 13).

#### BET analysis

Comparing the results from the BET analysis

for the primary and modified biomasses shows an increase in the surface area of the modified biomass due to the adsorption on clinoptilolite zeolite. The instrument received no response since the original biomass area was smaller than the minimum standard value of the BET test. After biomass correction, the specific surface area, average porosity diameter, and total porosity obtained from the BET test were  $9.688 \times 10^{-3} \text{ m}^2 \text{ g}^{-1}$ ,  $1.619 \times 10^2 \text{ nm}$ , and  $3.922 \times 10^{-4} \text{ cm}^3 \text{ g}^{-1}$ , respectively. As shown in Table 3, the total pore volume and average pore diameter of the modified zeolite adsorbent decreased significantly compared

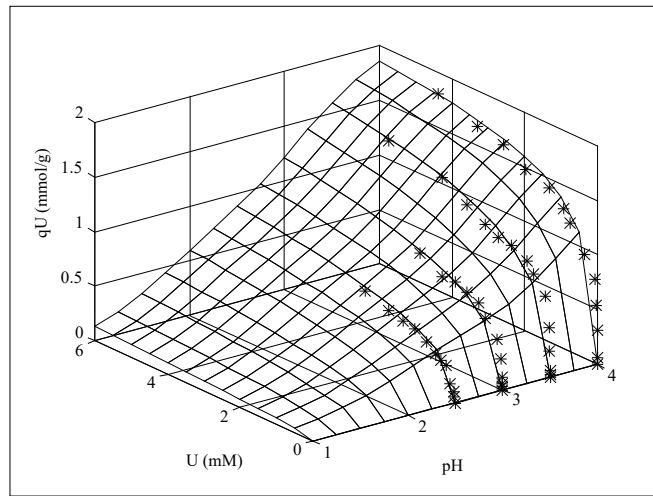


Fig 10: Uranium sorption isotherm experimental data and HIEM model regression at solution pH 2.5 – 4.0 and uranium concentration 0.0 – 6.0 mmol/L  
(\*) Experimental; (mesh) HIEM model

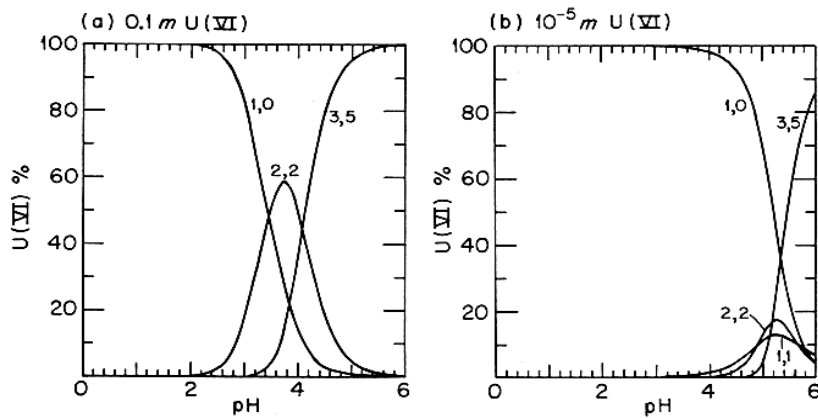


Fig. 11. Distribution of uranium hydrolysis products  
(1, 0):  $\text{UO}_2^{2+}$ ; (2, 2):  $(\text{UO}_2)_2(\text{OH})_2^{2+}$ ; (3, 5):  $(\text{UO}_2)_3(\text{OH})_5^{2+}$ .

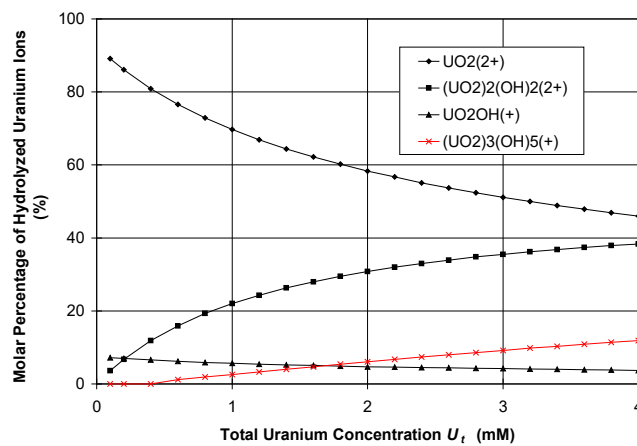


Fig. 12. Ionic composition of hydrolyzed uranium ions at pH 4.0

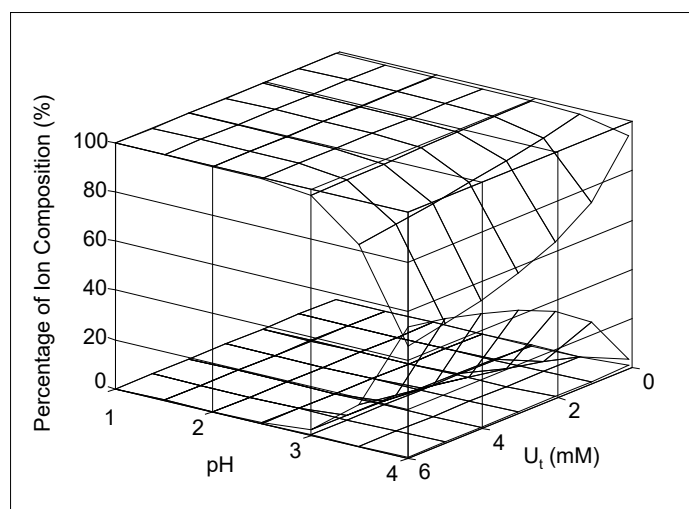


Fig. 13. Speciation of hydrolyzed ionic uranium

Top mesh:  $\text{UO}_2^{2+}$ ; Middle mesh:  $(\text{UO}_2^{2+})_2(\text{OH})_2^{2+}$ ; Bottom mesh:  $(\text{UO}_2^{2+})(\text{OH})^+$

Table 3. Comparison of total pore volume and average pore diameter of clinoptilolite zeolite with modified zeolite adsorbent

Samples	Total pore volume ( $\text{cm}^3/\text{gr}$ )	Surface area ( $\text{m}^2/\text{gr}$ )	average hole diameter (nm)
Clinoptilolite	0.1062	36.06	11.78
SC - Clinoptilolite	0.0673	12.67	2.26

to the clinoptilolite zeolite. Placing yeast molecules in the voids of the zeolite structure reduces the volume and diameter of the voids. Furthermore, since the placement of yeast molecules on the surface of the zeolite reduces the surface area of the zeolite with effective sites, the surface area of the modified zeolite is much smaller than that of the clinoptilolite zeolite. Therefore, this reduction in the surface area could be a justification for the proper modification of the raw zeolite surface and the placement of yeast molecules in the sites.

## CONCLUSIONS

This study indicates that SC yeast cells can be immobilized based on natural zeolite clinoptilolite which is suitable for adsorption of uranyl ions from aqueous solutions. The adsorption mechanism worked through forming a complex of polysaccharide and carboxyl groups on the cell wall of yeast by metal cations and ion exchange in the form of adsorption on the cell wall and deposition in the solution. Metal binding was also occurred extracellularly at the cell wall surface. Moreover, a genetic algorithm was applied to

obtain the optimal parameter values and consider the parameter estimation for the growth of SC in MBR. The results of the logistic kinetic model were in highly satisfactory agreement with the experimental data. The results of the discontinuous method demonstrated that the rate of sorption of uranyl ions by free yeast cells of SC is fast such that 85% of the total sorption occurs in the first 10 min of the contact, which allows for using economic reactors with small volume and high efficiency. The results of BET technique showed that the total pore volume and average pore diameter decreased with modified clinoptilolite zeolite, and the best pH for the adsorption process was found to be 4. When the pH is changed, the amount of adsorption in the free cell state decreases more than the amount of adsorption in the immobilized cells. The increase in the adsorption capacity of clinoptilolite after immobilization allows for a better use of this adsorbent in columnar systems. Due to the high mechanical strength of this adsorbent compared to free cells, it will also perform better in multiple desorption/adsorption periods in continuous systems [23, 24].

## CONFLICT OF INTEREST

All authors have no conflicts of interest to declare.

## ACKNOWLEDGEMENTS

None. No funding to declare.

## REFERENCES

- [1] Yang J, Volesky B. Modeling Uranium-Proton Ion Exchange in Biosorption. *Environmental Science & Technology*. 1999;33(22):4079-85.
- [2] Liu H, Wang R, Jiang H, Gong H, Wu X. Study on adsorption characteristics of uranyl ions from aqueous solutions using zirconium hydroxide. *Journal of Radioanalytical and Nuclear Chemistry*. 2015;308(1):213-20.
- [3] Behin J, Ghadamnan E, Kazemian H. Recent advances in the science and technology of natural zeolites in Iran. *Clay Minerals*. 2019;54(2):131-44.
- [4] Grant DC, Skriba MC, Saha AK. Removal of radioactive contaminants from West Valley waste streams using natural zeolites. *Environmental Progress*. 1987;6(2):104-9.
- [5] Ghasemi Mobtaker H, Kazemian H, Namdar MA, Malekinejad A, Pakzad MR. Ion Exchange Behavior of Zeolites A and P Synthesized Using Natural Clinoptilolite. *Iranian Journal of Chemistry and Chemical Engineering (IJCCE)*. 2008;27(2):111-7.
- [6] Jalali-Rad R, Ghafourian H, Asef Y, Dalir ST, Sahafipour MH, Gharanjik BM. Biosorption of cesium by native and chemically modified biomass of marine algae: introduce the new biosorbents for biotechnology applications. *Journal of Hazardous Materials*. 2004;116(1-2):125-34.
- [7] Shindo S, Takata S, Taguchi H, Yoshimura N. Development of novel carrier using natural zeolite and continuous ethanol fermentation with immobilized SC in a bioreactor. *Biotechnology Letters*. 2001;23(24):2001-4.
- [8] Fang X-H, Fang F, Lu C-H, Zheng L. Removal of Cs<sup>+</sup>, Sr<sup>2+</sup>, and Co<sup>2+</sup> Ions from the Mixture of Organics and Suspended Solids Aqueous Solutions by Zeolites. *Nuclear Engineering and Technology*. 2017;49(3):556-61.
- [9] Lan T, Feng Y, Liao J, Li X, Ding C, Zhang D, et al. Biosorption behavior and mechanism of cesium-137 on *Rhodospiridium fluviale* strain UA2 isolated from cesium solution. *Journal of Environmental Radioactivity*. 2014;134:6-13.
- [10] Zinicovscaia I, Safonov A, Boldyrev K, Gundorina S, Yushin N, Petuhov O, et al. Selective metal removal from chromium-containing synthetic effluents using *Shewanella xiamenensis* biofilm supported on zeolite. *Environmental Science and Pollution Research*. 2020;27(10):10495-505.
- [11] Aghadavoud A, Rezaee Ebrahim Saraee K, Shakur HR, Sayyari R. Removal of uranium ions from synthetic wastewater using ZnO/Na-clinoptilolite nanocomposites. *Radiochimica Acta*. 2016;104(11):809-19.
- [12] Bakatula EN, Mosai AK, Tutu H. Removal of uranium from aqueous solutions using ammonium-modified zeolite. *South African Journal of Chemistry*. 2015;68:165-71.
- [13] Fomina M, Gadd GM. Biosorption: current perspectives on concept, definition and application. *Bioresource Technology*. 2014;160:3-14.
- [14] Fadel M, Hassanein NM, Elshafei MM, Mostafa AH, Ahmed MA, Khater HM. Biosorption of manganese from groundwater by biomass of *Saccharomyces cerevisiae*. *HBRC Journal*. 2017;13(1):106-13.
- [15] Saifuddin NMaSD. Immobilization of SC onto cross-linked FA coated with magnetic nanoparticles for adsorption of Uranium(VI) ions. *Advances in Natural and Applied Sciences*. 2012;6:249-67.
- [16] Ayu ED, Halim L, Mellyanawaty M, Sudibyo H, Budhijanto W. The effect of natural zeolite as microbial immobilization media in anaerobic digestion at various concentrations of palm oil mill effluent (POME). *AIP Conference Proceedings* 2017. p. 110005.
- [17] Handley-Sidhu S, Mullan TK, Grail Q, Albadarneh M, Ohnuki T, Macaskie LE. Influence of pH, competing ions and salinity on the sorption of strontium and cobalt onto biogenic hydroxyapatite. *Scientific Reports*. 2016;6(1).
- [18] Zheng XY, Shen YH, Wang XY, Wang TS. Effect of pH on uranium(VI) biosorption and biomineralization by *Saccharomyces cerevisiae*. *Chemosphere*. 2018;203:109-16.
- [19] Emami Moghaddam SA, Harun R, Mokhtar MN, Zakaria R. Potential of Zeolite and Algae in Biomass Immobilization. *BioMed Research International*. 2018;2018:6563196.
- [20] Ma F, Dong B, Gui Y, Cao M, Han L, Jiao C, et al. Adsorption of Low-Concentration Uranyl Ion by Amidoxime Polyacrylonitrile Fibers. *Industrial & Engineering Chemistry Research*. 2018;57(51):17384-93.
- [21] Zhang W, Dong F, Liu M, Song H, Nie X, Huo T, et al. Reduction and Enrichment of Uranium after Biosorption on Inactivated *Saccharomyces cerevisiae*. *Polish Journal of Environmental Studies*. 2020;29(2):1461-72.
- [22] Peyvandi S, Faghihian H. Biosorption of uranyl ions from aqueous solution by *Saccharomyces cerevisiae* cells immobilized on clinoptilolite. *Journal of Radioanalytical and Nuclear Chemistry*. 2014;301(2):537-43.
- [23] Rosenberg E, Pinson G, Tsosie R, Tutu H, Cukrowska E. Uranium Remediation by Ion Exchange and Sorption Methods: A Critical Review. *Johnson Matthey Technology Review*. 2016;60(1):59-77.
- [24] Sadeghi M, Moghimifar Z, Javadian H, Jahanshahi M, Farsadrooh M. Treatment of nano-oil polluted wastewater in an expanded bed adsorption column based on carboxymethyl cellulose-cellulose-nickel composite beads. *Journal of Hazardous Materials*. 2021;417:126038.